A Generic and Robust System for Automated Patient-Specific Classification of ECG Signals

Turker Ince*, Serkan Kiranyaz, and Moncef Gabbouj, *Senior Member, IEEE*

Abstract—This paper presents a generic and patient-specific classification system designed for robust and accurate detection of ECG heartbeat patterns. The proposed feature extraction process utilizes morphological wavelet transform features, which are projected onto a lower dimensional feature space using principal component analysis, and temporal features from the ECG data. For the pattern recognition unit, feedforward and fully connected artificial neural networks, which are optimally designed for each patient by the proposed multidimensional particle swarm optimization technique, are employed. By using relatively small common and patient-specific training data, the proposed classification system can adapt to significant interpatient variations in ECG patterns by training the optimal network structure, and thus, achieves higher accuracy over larger datasets. The classification experiments over a benchmark database demonstrate that the proposed system achieves such average accuracies and sensitivities better than most of the current state-of-the-art algorithms for detection of ventricular ectopic beats (VEBs) and supra-VEBs (SVEBs). Over the entire database, the average accuracy–sensitivity performances of the proposed system for VEB and SVEB detections are 98.3%–84.6% and 97.4%–63.5%, respectively. Finally, due to its parameter-invariant nature, the proposed system is highly generic, and thus, applicable to any ECG dataset.

Index Terms—Biomedical signal classification, evolutionary neural networks, multidimensional (MD) search, particle swarm optimization (PSO).

I. INTRODUCTION

EACH individual heartbeat in the cardiac cycle of the recorded ECG waveform shows the time evolution of the heart's electrical activity, which is made of distinct electrical depolarization–repolarization patterns of the heart. Any disorder of heart rate or rhythm, or change in the morphological pattern, is an indication of an arrhythmia, which could be detected by analysis of the recorded ECG waveform. Real-time automated ECG analysis in clinical settings is of great assistance to clinicians in detecting cardiac arrhythmias, which often arise as a consequence of a cardiac disease, and may be life-threatening and require immediate therapy. However, automated classification of ECG beats is a challenging problem as the morphological and temporal characteristics of ECG

*T. Ince is with the Computer Engineering Department, Izmir University of Economics, Izmir 35330, Turkey (e-mail: turker.ince@ieu.edu.tr).

S. Kiranyaz and M. Gabbouj are with the Department of Signal Processing, Tampere University of Technology, Tampere 33101, Finland (e-mail: serkan.kiranyaz@tut.fi; moncef.gabbouj@tut.fi).

signals show significant variations for different patients and under different temporal and physical conditions [1]. Many algorithms for automatic detection and classification of ECG heartbeat patterns have been presented in the literature, including signal processing techniques such as frequency analysis [2], wavelet transform [3], [4], filter banks [5], statistical [6] and heuristic approaches [7], hidden Markov models [8], support vector machines [9], artificial neural networks (ANNs) [10], and mixture-of-experts method [11]. In general, ECG classifier systems based on past approaches have not performed well in practice because of their important common drawback of having an inconsistent performance when classifying a new patient's ECG waveform. This makes them unreliable to be widely used clinically, and causes severe degradation in their accuracy and efficiency for larger databases [12], [13]. Moreover, the Association for the Advancement of Medical Instrumentation (AAMI) provides standards and recommended practices for reporting performance results of automated arrhythmia detection algorithms [14]. However, despite quite many ECG classification methods proposed in the literature, only few [11], [15], [16] have, in fact, used the AAMI standards as well as the complete data from the benchmark MIT/BIH arrhythmia database.

The performance of ECG pattern classification strongly depends on the characterization power of the features extracted from the ECG data and the design of the classifier (classification model or network structure and parameters). Due to its time–frequency localization properties, the wavelet transform is an efficient tool for analyzing nonstationary ECG signals [17]. The wavelet transform can be used to decompose an ECG signal according to scale, thus allowing separation of the relevant ECG waveform morphology descriptors from the noise, interference, baseline drift, and amplitude variation of the original signal. Several researchers have previously used the wavelet transform coefficients at the appropriate scales as morphological feature vectors rather than the original signal time series and achieved good classification performance [3], [4]. Accordingly, in the current paper, the proposed feature extraction technique employs the translation-invariant dyadic wavelet transform (TI-DWT) in order to effectively extract the morphological information from ECG data. Furthermore, the dimension of the input morphological feature vector is reduced by projecting it onto a lower dimensional feature space using principal component analysis (PCA) in order to significantly reduce redundancies in such a high-dimensional data space. The lower dimensional morphological feature vector is then combined with two critical temporal features related to interbeat time interval to improve accuracy and robustness of classification, as suggested by the results of previous studies [15].

ANNs are powerful tools for pattern recognition as they have the capability to learn complex, nonlinear surfaces among different classes, and such ability can therefore be the key for ECG beat recognition and classification [18]. Although many promising ANN-based techniques have been applied to ECG signal classification [18]–[21], the global classifiers based on a static (fixed) ANN have not performed well in practice. On the other hand, algorithms based on patient-adaptive architecture have demonstrated significant performance improvement over conventional global classifiers [11], [13], [16]. Among all, one particular approach, a personalized ECG heartbeat pattern classifier based on evolvable block-based neural networks (BbNNs) using *Hermite* transform coefficients [16], achieved such a performance that is significantly higher than the others. Although this recent work clearly demonstrates the advantage of using evolutionary ANNs, which can be automatically designed according to the problem (patient's ECG data), serious drawbacks and limitations can also be observed. For instance, there are around 10–15 parameters/thresholds that needed to be set empirically with respect to the dataset used, and this obviously brings about the issue of robustness when it is used for a different database. Another drawback can occur due to the specific ANN structure proposed, i.e., the BbNN, which requires equal sizes for input and output layers. Even more critical is the back-propagation (BP) method, used for training, and genetic algorithm (GA), for evolving the network structure, as both have certain deficiencies [22]. In particular, the BP most likely gets trapped into a local minimum, making it entirely dependent on the initial (weight) settings.

In order to address such deficiencies and drawbacks, in this paper, we propose a multidimensional particle swarm optimization (MD PSO) technique, which automatically designs the optimal ANNs [both network structure and connection weights with respect to the training mean squarred error (MSE)] specifically for each patient and according to the patient's ECG data. In contrast to the specific BbNN structure used in [16] with the aforementioned problems, MD PSO is used to evolve traditional ANNs, and so the focus is particularly drawn on automatic design of the multilayer perceptrons (MLPs). This evolutionary operator makes the proposed system *generic*, i.e., no assumption is made about the number of (hidden) layers, and in fact, none of the network properties (e.g., feedforward or not, differentiable activation function or not, etc.) is an inherent constraint. As long as the potential network configurations are transformed into a hash (dimension) table with a proper hash function where indexes represent the solution space dimensions of the particles, MD PSO can seek both positional and dimensional optima in an interleaved PSO process. The optimum dimension found corresponds to a distinct ANN architecture where the network parameters (connections, weights, and biases) can be resolved from the positional optimum reached on that dimension. Our earlier work on detection of premature ventricular contractions (PVCs) demonstrated performance improvement of the proposed approach over conventional techniques [23]. Moreover, we aim to achieve a high level of *robustness* with respect to the variations of the dataset, since the proposed system is designed with a minimum set of parameters and in such a way
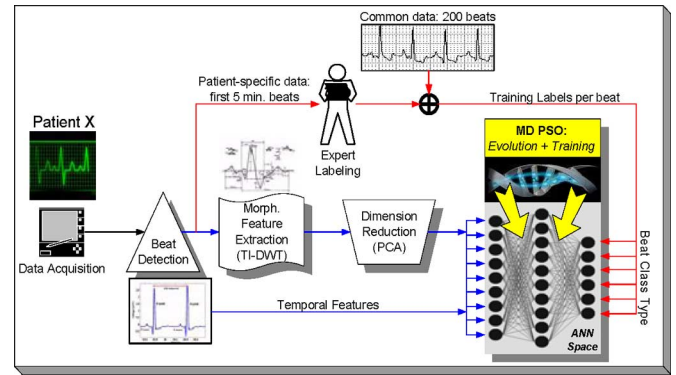

Fig. 1. Patient-specific training process of the proposed ECG classification system.

that their significant variations should not show a major impact on the overall performance. Above all, using standard ANNs such as traditional MLPs, instead of specific architectures (e.g., BbNN in [16]) further contributes to the generic nature of the proposed system, and in short, all these objectives are meant to make it applicable to any ECG dataset without any modifications (such as tuning the parameters or changing the feature vectors, ANN types, etc.). The overview of the proposed system is shown in Fig. 1.

The rest of the paper is organized as follows. Section II outlines the ECG dataset used in this study and provides a detailed description of the feature extraction methodology for the proposed patient-specific heartbeat classification system. MD PSO and its application over the automatic ANN design are presented in Section III. In Section IV, the optimality, performance, and robustness of the proposed classifier are evaluated over the MIT/BIH arrhythmia database using standard performance metrics and the results are compared with previously published work. Finally, Section V concludes the paper.

II. ECG DATA PROCESSING

A. ECG Data

In this study, the MIT/BIH arrhythmia database [24] is used for training and performance evaluation of the proposed patient-specific ECG classifier. The database contains 48 records, each containing two-channel ECG signals for 30 min duration selected from 24-h recordings of 47 individuals. Continuous ECG signals are bandpass-filtered at 0.1–100 Hz and then digitized at 360 Hz. The database contains annotation for both timing information and beat class information verified by independent experts. In the current paper, so as to comply with the AAMI ECAR-1987 recommended practice [14], we used 44 records from the MIT/BIH arrhythmia database, excluding 4 records that contain paced heartbeats. The first 20 records (numbered in the range of 100–124), which include representative samples of routine clinical recordings, are used to select representative beats to be included in the common training data. The remaining 24 records (numbered in the range of 200–234) contain ventricular, junctional, and supraventricular arrhythmias. A total of 83 648 beats from all 44 records are used as test patterns for performance evaluation. AAMI recommends that each ECG
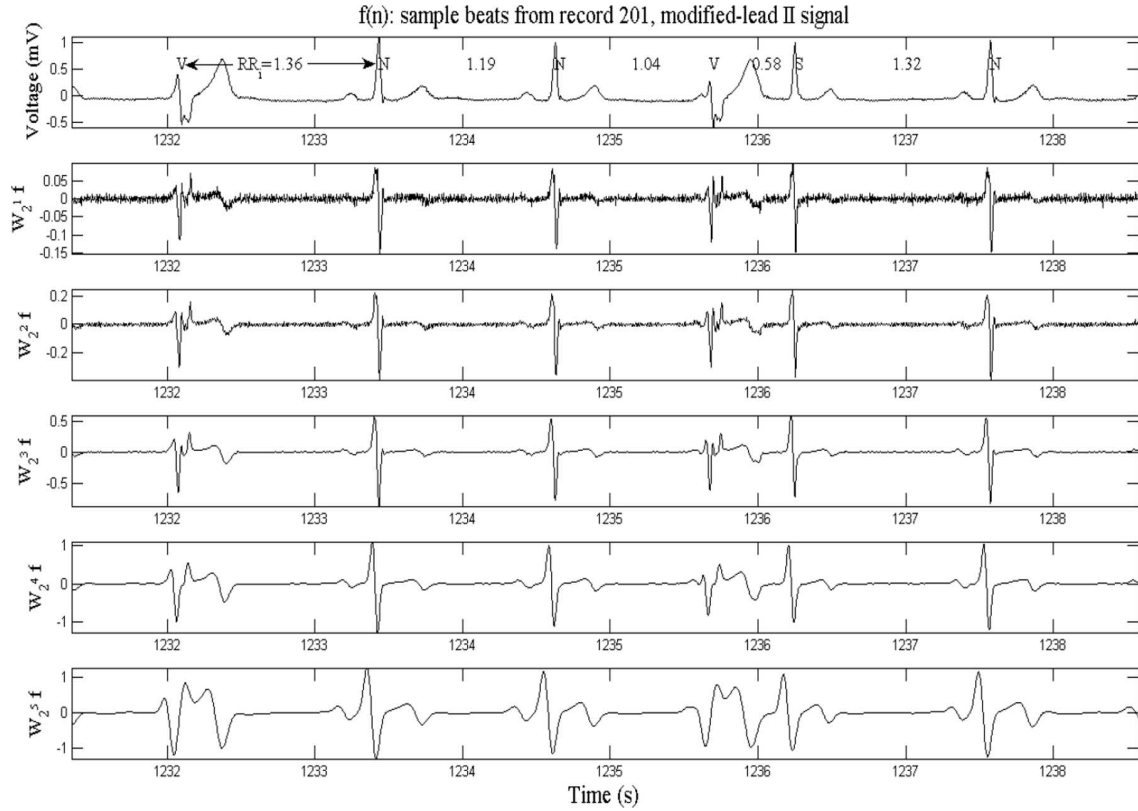
Fig. 2.   Sample beat waveforms, including normal (N), PVC (V), and APC (S) AAMI heartbeat classes, selected from record 201 modified-lead II from the MIT/BIH arrhythmia database and corresponding TI-DWT decompositions for the first five scales.

beat be classified into the following five heartbeat types: N (beats originating in the sinus mode), S (supraventricular ectopic beats (SVEBs)), V (ventricular ectopic beats (VEBs)), F (fusion beats), and Q (unclassifiable beats). For all records, we used the modified-lead II signals and utilized the labels to locate beats in ECG data. The beat detection process is beyond the scope of this paper, as many highly accurate ($>99\%$) beat detection algorithms have been reported in literature [17], [25].

B. Feature Extraction Methodology

As suggested by the results from previous works [10], [11], [15], both morphological and temporal features are extracted and combined into a single feature vector for each heartbeat to improve accuracy and robustness of the proposed classifier. The wavelet transform is used to extract morphological information from the ECG data. The time-domain ECG signatures were first normalized by subtracting the mean voltage before transforming into time-scale domain using the DWT. According to wavelet transform theory, the multiresolution representation of the ECG signal is achieved by convolving the signal with scaled and translated versions of a mother wavelet. For practical applications, such as processing of sampled and quantized raw ECG signals, the discrete wavelet transform can be computed by scaling the wavelet at the dyadic sequence $\left(2^j\right)_{j \in Z}$ and translating it on a dyadic grid whose interval is proportional to 2^{-j}. The discrete WT is not only complete but also nonredundant unlike the continuous WT. Moreover, the wavelet transform of a discrete

signal can be efficiently calculated using the decomposition by a two-channel multirate filter bank (the pyramid decomposition). However, due to the rate-change operators in the filter bank, the discrete WT is not time-invariant but actually very sensitive to the alignment of the signal in time [26].

To address the time-varying problem of wavelet transforms, Mallat and Zhong proposed a new algorithm for wavelet representation of a signal, which is invariant to time shifts [27]. According to this algorithm, which is called a TI-DWT, only the scale parameter is sampled along the dyadic sequence $\left(2^j\right)_{j \in Z}$ and the wavelet transform is calculated for each point in time. TI-DWTs pioneered by Mallat and Zhong have been successfully applied to pattern recognition [27]. The fast TI-DWT algorithm, whose computational complexity is $O(N \log N)$, can be implemented using a recursive filter tree architecture [27]. In this study, we selected a quadratic spline wavelet with compact support and one vanishing moment, as defined in [27]. The same wavelet function has already been successfully applied to QRS detection in [17], achieving a 99.8% QRS detection rate for the MIT/BIH arrhythmia database. In the proposed ECG classification system, using a wavelet-based beat detector, such as in [17], allows the same wavelet transform block to operate directly on the raw input ECG signal for beat detection and then morphological feature extraction, thus making the system more efficient and robust.

Fig. 2 shows sample beat waveforms, including normal (N), premature ventricular contraction (V), and atrial premature contraction (S) AAMI heartbeat classes, selected from record
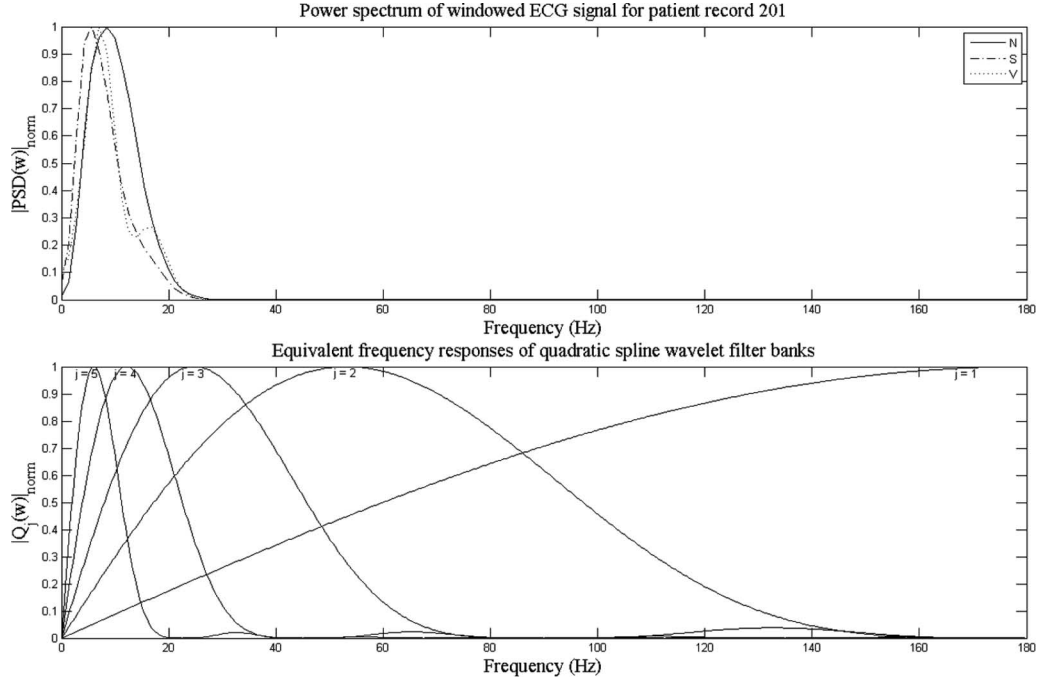
Fig. 3. Power spectrum of windowed ECG signal from record 201 for normal (N), PVC (V), and APC (S) AAMI heartbeat classes, and equivalent frequency responses of FIR digital filters for a quadratic spline wavelet at 360 Hz sampling rate.

201, modified-lead II from the MIT/BIH arrhythmia database, and their corresponding TI-DWT decompositions computed for the first five scales. While wavelet-based morphological features provide effective discrimination capability between normal and some abnormal heartbeats (i.e., PVC beats), two temporal features (i.e., the R-R time interval and R-R time interval ratio) contribute to the discriminating power of wavelet-based features, especially in discriminating morphologically similar heartbeat patterns (i.e., normal and APC beats).

In Fig. 3 (top), the estimated power spectrum of windowed ECG signal (a 500-ms-long *Hanning* window is applied before fast Fourier transform (FFT) to suppress high-frequency components due to discontinuities in the end-points) from record 201 is plotted for N, V, and S beats, while equivalent frequency responses of finite-impulse response (FIR) filters, $Q_j(w)$, for the first five scales at the native 360 Hz sampling frequency of the MIT/BIH data are illustrated in the bottom part of the figure. After analyzing the DWT decompositions of different ECG waveforms in the database, and according to the power spectra of ECG signal (the QRS complex, the P- and T-waves), noise, and artifact in [28], we selected $W_{2^4}f$ (at scale 2^4) signal as morphological features of each heartbeat waveform. Based on the -3 dB bandwidth of the equivalent $Q_4(w)$ filter (3.9–22.5 Hz) in Fig. 3 (bottom), $W_{2^4}f$ signal is expected to contain most of QRS complex energy and the least amount of high-frequency noise and low-frequency baseline wander. The fourth scale decomposition together with RR-interval timing information was previously shown to be the best performing feature set for DWT-based PVC beat classification in [4]. Therefore, a 180-sample morphological feature vector is extracted per heartbeat from DWT of ECG signal at scale 2^4 by selecting a 500 ms window centered at the R-peak (found by using the beat

annotation file). Each feature vector is then normalized to have a zero mean and a unit variance to eliminate the effect of dc offset and amplitude biases.

C. Preprocessing by PCA

The wavelet-based morphological features in the training set are postprocessed using PCA to reduce dimensionality (and redundancy) of input feature vectors. PCA, also known as the Karhunen–Loéve transform (KLT), is a well-known statistical method that has been used for data analysis, data compression, redundancy and dimensionality reduction, and feature extraction. PCA is the optimal linear transformation, which finds a projection of the input pattern vectors onto a lower dimensional feature space that retains the maximum amount of energy among all possible linear transformations of the pattern space. To describe the basic procedure of PCA, let F be a feature matrix of size $K \times N$, whose rows are wavelet features of size $1 \times N$, each belonging to one of K heartbeats in the training data. First, the covariance matrix C_F of this feature matrix is computed as

$$C_F = E\left\{(F - m)(F - m)^t\right\} \qquad (1)$$

where m is the mean pattern vector. From the eigen-decomposition of C_F, which is a $K \times K$ symmetric and positive-definite matrix, the principal components taken as the eigenvectors corresponding to the largest eigenvalues are selected, and the morphological feature vectors are then projected onto these principal components (KL basis functions). In this paper, nine principal components, which contain about 95% of overall energy in the original feature matrix, are selected to form a resultant compact morphological feature vector for each heartbeat signal. In this case, the PCA reduced the dimensionality of
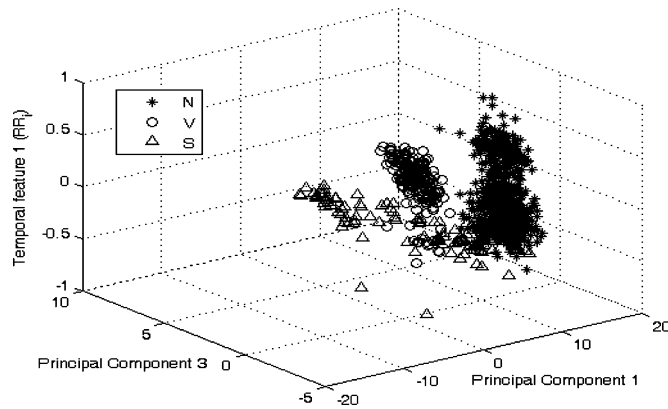
Fig. 4. Scatter plot of normal (N), PVC (V), and APC (S) beats from record 201 in terms of the first and third principal components and RR_i time interval.

morphological features by a factor of 20. Fig. 4 shows a scatter plot of normal, PVC, and APC beats from record 201 in terms of the first and third principal components and interbeat time interval. It is worth noting that dimensionality reduction of the input information improves efficiency of the learning for an NN classifier due to a smaller number of input nodes [29].

The data used for training the individual patient classifier consist of two parts: global (common to each patient) and local (patient specific) training patterns. While patient-specific data contain the first 5-min segment of each patient's ECG record and are used as part of the training data to perform patient adaptation, the global dataset contains a relatively small number of representative beats from each class in the training files and helps the classifier learn other arrhythmia patterns that are not included in the patient-specific data. This practice conforms to the AAMI-recommended procedure allowing the usage of at most 5-min section from the beginning of each patient's recording for training [14].

III. MD PSO TECHNIQUE FOR AUTOMATIC ANN DESIGN

As mentioned earlier, evolutionary ANNs are used for the classification of ECG data from each individual patient in the database. In this section, the MD PSO technique, which is developed for evolving ANNs, will be introduced first, and we shall next present its application for evolving the feedforward ANNs.

A. MD PSO Algorithm

The behavior of a single organism in a swarm is often insignificant but their collective and social behavior is of paramount importance. The PSO was introduced by Kennedy and Eberhart in 1995 as a population-based stochastic search and optimization process [30]. It is originated from the computer simulation of the individuals (particles or living organisms) in a bird flock or fish school, which basically shows a natural behavior when they search for some target (e.g., food). In the basic PSO algorithm, the particles are initially distributed randomly over the search space with a random velocity and the goal is to converge to the global optimum (according to a given fitness score) of a

function or a system. Each particle keeps track of its position in the search space and its best solution (i.e., lowest fitness score) achieved so far. This is the personal best value (the so-called *pbest*) and the PSO process also keeps track of the global best solution so far achieved by the swarm with its particle index (the so-called *gbest*). So during their journey with discrete-time iterations, the velocity of each particle in the next iteration is computed by the best position of the swarm (best personal position of the particle *gbest* as the *social* component), the best personal position of the particle (*pbest* as the *cognitive* component), and its current velocity (the *memory* term). Both *social* and *cognitive* components contribute randomly to the position of the particle in the next iteration. In principle, PSO follows the same path of the other evolutionary algorithms (EAs) such as GA, genetic programming (GP), evolutionary strategies (ES), and evolutionary programming (EP). The common point of all is that EAs are in population-based nature, and thus, they can avoid being trapped in a local optimum. Thus, they can find the optimum solutions; however, this is never guaranteed.

Instead of operating at a fixed dimension N, the MD PSO algorithm is designed to seek both positional and dimensional optima within a dimension range ($D_{\min} \leq N \leq D_{\max}$). In order to accomplish this, each particle has two sets of components, each of which has been subjected to two independent and consecutive processes. The first one is a regular positional PSO, i.e., the traditional velocity updates and due positional shifts in N-dimensional search (solution) space. The second one is a dimensional PSO, which allows the particle to navigate through a range of dimensions. Accordingly, each particle keeps track of its last position, velocity, and personal best position (*pbest*) in a particular dimension so that when it revisits that same dimension at a later time, it can perform its regular "positional" fly using this information. The dimensional PSO process of each particle may then move the particle to another dimension where it will remember its positional status and keep "flying" within the positional PSO process in this dimension, and so on. The swarm, on the other hand, keeps track of the *gbest* particles in all dimensions, each of which respectively indicates the best (global) position so far achieved and can thus be used in the regular velocity update equation for that dimension. Similarly, the dimensional PSO process of each particle uses its personal best dimension in which the personal best fitness score has so far been achieved. Finally, the swarm keeps track of the global best dimension *dbest* among all the personal best dimensions. The *gbest* particle in *dbest* dimension represents the optimum solution and dimension, respectively. The details and the pseudocode of the MD PSO algorithm are presented in the Appendix.

B. MD PSO for Evolving ANNs

As a stochastic search process in an MD space, MD PSO seeks (near-)optimal (with respect to the training error) networks in an architecture space, which can be defined by any type of ANNs with any properties. All network configurations in the architecture space are enumerated into a (dimensional) hash table with a proper hash function, which basically ranks the networks with respect to their complexity, i.e., associates higher hash indexes

to networks with higher complexity. MD PSO can then use each index as a unique dimension of the search space where particles can make interdimensional navigations to seek an optimum dimension (*dbest*) and the optimum solution on that dimension $x\hat{y}^{dbest}$. As mentioned earlier, the former corresponds to the optimal architecture and the latter encapsulates the (optimum) network parameters (connections, weights, and biases).

In this section, we apply MD PSO technique for evolving fully connected, feedforward ANNs, or the so-called MLPs. As mentioned earlier, the reasoning behind this choice is that MLP is the most widely used in this field and so our aim is to show that a superior performance as in [16] can also be achieved without using such specific ANN structures. MD PSO can evolve any MLP type, and thus, the architecture space can be defined over a wide range of configurations, i.e., from a single-layer perceptron (SLP) to complex MLPs with many hidden layers. Suppose for the sake of simplicity, a range is defined for the minimum and maximum number of layers, $\{L_{\min}, L_{\max}\}$ and the number of neurons for hidden layer l $\{N_{\min}^l, N_{\max}^l\}$. Without loss of generality, assume that the size of both input and output layers is determined by the problem, and hence, fixed. As a result, the architecture space can now be defined only by two range arrays, $R_{\min} = \{N_I, N_{\min}^1, \ldots, N_{\min}^{L_{\max}-1}, N_O\}$ and $R_{\max} = \{N_I, N_{\max}^1, \ldots, N_{\max}^{L_{\max}-1}, N_O\}$, one for the minimum and the other for the maximum number of neurons allowed for each layer of a MLP. The size of both arrays is naturally $L_{\max} + 1$ where corresponding entries define the range of the lth hidden layer for all those MLPs, which can have an lth hidden layer. The size of input and output layers, $\{N_I, N_O\}$, is fixed and remains the same for all configurations in the architecture space within which any l-layer MLP can be defined provided that $L_{\min} \leq l \leq L_{\max}$. $L_{\min} \geq 1$ and $L_{\max}$ can be set to any meaningful value for the problem at hand. The hash function then enumerates all potential MLP configurations into hash indexes, starting from the simplest MLP with $L_{\min} - 1$ hidden layers, each of which has a minimum number of neurons given by $R_{\min}$, to the most complex network with $L_{\max} - 1$ hidden layers, each of which has a maximum number of neurons given by $R_{\max}$.

Let N_h^l be the number of hidden neurons in layer l of a MLP with input and output layer sizes N_I and N_O, respectively. The input neurons are merely fan-out units since no processing takes place. Let F be the activation function applied over the weighted inputs plus a bias, which is given as follows:

$$y_k^{p,l} = F(s_k^{p,l}), \text{ where } s_k^{p,l} = \sum_j w_{jk}^{l-1} y_j^{p,l-1} + \theta_k^l \quad (2)$$

where $y_k^{p,l}$ is the output of the kth neuron of the lth hidden/output layer when the pattern p is fed, w_{jk}^{l-1} is the weight from the jth neuron in layer $(l-1)$ to the kth neuron in layer l, and θ_k^l is the bias value of the kth neuron of the lth hidden/output layer. The cost function under which optimality is sought is the training MSE formulated as

$$\text{MSE} = \frac{1}{2PN_O} \sum_{p \in T} \sum_{k=1}^{N_O} \left(t_k^p - y_k^{p,O} \right)^2 \quad (3)$$

where t_k^p is the target (desired) output and $y_k^{p,O}$ is the actual output from the kth neuron in the output layer, $l = O$, for pattern p in the training set T with size P, respectively. At time t, suppose the particle a in the swarm $\xi = \{x_1, \ldots, x_a, \ldots, x_S\}$ has the positional component formed as $xx_a^{xd_a(t)}(t) = \{\{w_{jk}^0\}, \{w_{jk}^1\}, \{\theta_k^1\}, \{w_{jk}^2\}, \{\theta_k^2\}, \ldots, \{w_{jk}^{O-1}\}, \{\theta_k^{O-1}\}, \{\theta_k^O\}\}$, where $\{w_{jk}^l\}$ and $\{\theta_k^l\}$ represent the sets of weights and biases of the layer l. Note that the input layer ($l = 0$) contains only weights whereas the output layer ($l = O$) has only biases. By means of such a direct encoding scheme, a particle a in the swarm represents all potential network parameters of the MLP architecture at the dimension (hash index) $xd_a(t)$. As mentioned earlier, the dimension range $D_{\min} \leq xd_a(t) \leq D_{\max}$, where MD PSO particles can make interdimensional jumps, is determined by the architecture space defined. Apart from the regular limits such as (positional) velocity range $\{V_{\min}, V_{\max}\}$ and dimensional velocity range $\{VD_{\min}, VD_{\max}\}$, the data space can also be limited with some practical range, i.e., $X_{\min} < xx_a^{xd_a(t)}(t) < X_{\max}$. In short, only some meaningful boundaries should be defined in advance for an MD PSO process, as opposed to other GA-based methods, which use several parameters, thresholds, and some other (alien) techniques (e.g., simulated annealing (SA), BP, etc.) in a complex process. Setting MSE in (3) as the fitness function enables MD PSO to perform *evolutions* of both network parameters and architectures within its native process.

IV. EXPERIMENTAL RESULTS

In this section, we shall first demonstrate the *optimality* of the networks (with respect to the training MSE as in (3)), which are automatically evolved by the MD PSO method according to the training set of an individual patient record in the benchmark database. We shall then present the overall results obtained from the ECG classification experiments and perform comparative evaluations against several state-of-the-art techniques in this field. Finally, the robustness of the proposed system against variations of major parameters will be evaluated.

A. MD PSO Optimality Evaluation

In order to determine which network architectures are optimal (whether it is global or local) for a particular problem, we apply exhaustive BP training over every network configuration in the architecture space defined. As mentioned earlier, BP is a gradient-descent algorithm, and thus, for a single run, it is susceptible to getting trapped to the nearest local minimum. However, performing it a large number of times (e.g., $K = 500$) with randomized initial parameters eventually increases the chance of converging to (a close vicinity of) the global minimum of the fitness function. Note that even though K is kept quite high, there is still no guarantee of converging to the global optimum with BP; however, the idea is to obtain the "trend" of best performances achievable with every configuration under equal training conditions. In this way, the optimality of the networks evolved by MD PSO can be justified under the assumed criterion.
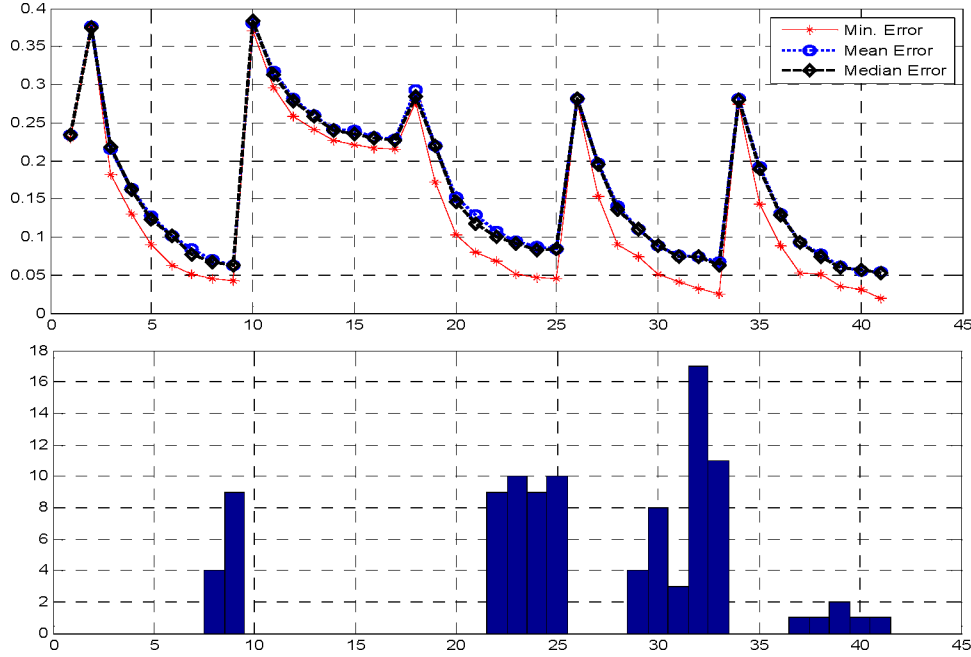
Fig. 5. Error (MSE) statistics from exhaustive BP training (top) and *dbest* histogram from 100 MD PSO evolutions (bottom) for patient record 222.

Due to the reasoning given earlier, the architecture space is defined over MLPs (possibly including one SLP) with the following activation function: *hyperbolic tangent* $(\tanh(x) = (e^x - e^{-x})/(e^x + e^{-x}))$. The input and output layer sizes are determined by the problem. We use a learning parameter for BP as $\lambda = 0.001$ and iteration number is 10 000. We kept the default PSO parameters for MD PSO with a swarm size $S = 100$, and velocity ranges are empirically set as $V_{max} = -V_{min} = X_{max}/2$ and $VD_{max} = -VD_{min} = D_{max}/2$. The dimension range is determined by the architecture space defined and the position range is set as $X_{max} = -X_{min} = 2$. Unless stated otherwise, these parameters are used in all experiments presented in this section.

In order to show the optimality of the network configurations evolved by MD PSO with respect to the MSE criterion, we first use the "limited" architecture space with 41 ANNs (R^1 : $R^1_{min} = \{N_I, 1, 1, N_O\}$ and $R^1_{max} = \{N_I, 8, 4, N_O\}$) containing the simplest one-, two-, or three-layer MLPs with $L^1_{min} = 1$, $L^1_{max} = 3$, and $N_I = 11, N_O = 5$. We then select one of the most challenging records among MIT/BIH arrhythmia database, belonging to the patient record 222. For this record, we perform 100 MD PSO runs with 100 particles, each of which terminates at the end of 1000 epochs (iterations). At the end of each run, the best fitness score (minimum MSE) achieved $f(x\hat{y}^{dbest})$ by the particle with the index *gbest(dbest)* at the optimum dimension *dbest* is stored. The histogram of *dbest*, which is a hash index indicating a particular network configuration in R^1, eventually provides the crucial information about the (near-)optimal configuration(s).

Fig. 5 shows *dbest* histogram and the error statistics plot from the exhaustive BP training the data of patient record 222. From the minimum (mean-squared) error (mMSE) plot of the exhaustive BP training on top, it is clear that only four distinct sets of

network configurations can achieve training mMSEs below 0.1. The corresponding indexes (dimensions) to these four optimal networks are $dbest = 9, 25, 33$, and 41, where MD PSO managed to evolve either to them or to a neighbor (near-optimal) configuration. MD PSO can, in fact, achieve the best (lowest) training MSEs for two sets of configurations: $dbest = 33$ and 41 (including their close neighbors). These are three-layer MLPs: $dbest = 33$ is for $11 \times 8 \times 3 \times 5$ and $dbest = 41$ is for $11 \times 8 \times 4 \times 5$. All MD PSO runs evolved either to $dbest = 25$ (corresponding to configuration $11 \times 8 \times 2 \times 5$) or to its neighbors and performed slightly worse than the best configurations. MD PSO runs, which evolved to the simplest MLPs with single hidden layer (i.e., $dbest = 8$ and 9 are for the MLPs $11 \times 7 \times 5$ and $11 \times 8 \times 5$), achieved the worst *mMSE, about 15% higher than for dbest* = 33 and 41. The reason of MD PSO evolutions to those slightly worse configurations (for $dbest = 25$ and particularly for $dbest = 9$) is that MD PSO or PSO, in general, performs better in low dimensions. Furthermore, premature convergence is still a problem in PSO when the search space is in high dimensions [31]. Therefore, MD PSO naturally favors a low-dimension solution when it exhibits a competitive performance compared to a higher dimension counterpart. Such a natural tendency eventually yields the evolution process to compact network configurations in the architecture space rather than the complex ones, as long as optimality prevails.

B. Classification Performance

We performed classification experiments on 44 records of the MIT/BIH arrhythmia database, which includes a total of 100 558 beats to be classified into five heartbeat types following the AAMI convention. For the classification experiments in this paper, the common part of the training dataset contains a total

TABLE I
SUMMARY TABLE OF BEAT-BY-BEAT CLASSIFICATION RESULTS FOR ALL 44
RECORDS IN MIT/BIH ARRHYTHMIA DATABASE

		Classification Result				
		N	S	V	F	Q
Ground Truth	N	73019 (40532)	991 (776)	513 (382)	98 (56)	29 (20)
	S	686 (672)	1568 (1441)	205 (197)	5 (5)	6 (5)
	V	462 (392)	333 (299)	4993 (4022)	79 (75)	32 (32)
	F	168 (164)	28 (26)	48 (46)	379 (378)	2 (2)
	Q	8 (6)	1 (0)	3 (1)	1 (1)	1 (0)

Classification results for the testing dataset only (24 records from range 200–234) are shown in parenthesis.

of 245 representative beats, including 75 from each type-N, -S, and -V beats, and all (13) type-F and (7) type-Q beats, *randomly* sampled from each class from the first 20 records (picked from the range 100–124) of the MIT/BIH database. The patient-specific training data include the beats from the first 5 min of the corresponding patient's ECG record. Patient-specific feedforward MLP networks are trained with a total of 245 common training beats and a variable number of patient-specific beats depending on the patient's heart rate, so only less than 1% of the total beats are used for training each neural network. The remaining beats (25 min) of each record, in which 24 out of 44 records are completely new to the classifier, are used as test patterns for performance evaluation.

Table I summarizes beat-by-beat classification results of ECG heartbeat patterns for all test records. Classification performance is measured using the four standard metrics found in the literature [11]: classification accuracy (*Acc*), sensitivity (*Sen*), specificity (*Spe*), and positive predictivity (*Ppr*). While accuracy measures the overall system performance over all classes of beats, the other metrics are specific to each class and they measure the ability of the classification algorithm to distinguish certain events (i.e., VEBs or SVEBs) from nonevents (i.e., non-VEBs or non-SVEBs). The respective definitions of these four common metrics using true positive (*TP*), true negative (*TN*), false positive (*FP*), and false negative (*FN*) are as follows: *accuracy* is the ratio of the number of correctly classified patterns to the total number of patterns classified: $Acc = (TP+TN)/(TP+TN+FP+FN)$; *sensitivity* is the rate of correctly classified events among all events: $Sen = TP/(TP + FN)$; *specificity* is the rate of correctly classified nonevents among all nonevents: $Spe = TN/(TN + FP)$; and *positive predictivity* is the rate of correctly classified events in all detected events: $Ppr = TP/(TP + FP)$. Since there is a large variation in the number of beats from different classes in the training/testing data (i.e., 39465/50354 type-N, 1277/5716 type-V, and 190/2571 type-S beats), sensitivity, specificity, and positive predictivity are more relevant performance criteria for medical diagnosis applications.

The proposed system is compared with three existing algorithms, [11], [15], and [16], which comply with the AAMI standards and use *all* records from the MIT/BIH arrhythmia database. For comparing the performance results, the problem of VEB and SVEB detection is considered individually. The VEB and SVEB classification results of the proposed technique over all 44 records are summarized in Table II. The performance results for VEB detection in the first four rows of Table II are based on 11 test recordings (200, 202, 210, 213, 214, 219, 221, 228, 231, 233, and 234) that are common to all four methods. For SVEB detection, comparison results are based on 14 common recordings (with the addition of records 212, 222, and 232) between the proposed technique and the methods in [15] and [16]. Several interesting observations can be made from these results. First, for SVEB detection, sensitivity and positive predictivity rates are comparably lower than VEB detection, while a high specificity performance is achieved. The reason for the worse classifier performance in detecting SVEBs is that SVEB class is underrepresented in the training data, and hence, more SVEB beats are misclassified as normal beats. Overall, the performance of the proposed technique in VEB and SVEB detection is significantly better than [11] and [15] for all measures and is comparable to the results obtained with evolvable BbNNs in [16]. Moreover, it is observed that the proposed classifier achieves comparable performance over the training and testing set of patient records. It is worth noting that the number of training beats used for each patient's classifier was less than 2% of all beats in the training dataset and the resulting classifiers designed by the MD PSO process have improved generalization ability, i.e., the same low number of design parameters are used for all networks.

C. Robustness

In order to investigate the robustness of the proposed technique against the variations of the few PSO parameters used, such as the swarm size S, the iteration number I, and to evaluate the effect of the architecture space (and hence, the characteristics of the ANNs used), we performed four classification experiments over the MIT/BIH arrhythmia database (I–IV) and their classification accuracy results per VEB and SVEB are presented in Table III. Experiments I–III are performed over the same architecture space, with one-, two-, and three-layer MLP architectures defined by $R_{\min}^1 = \{11, 8, 4, 5\}$, $R_{\max}^1 = \{11, 16, 8, 5\}$. Between I and II, the swarm size, and between II and III, the iteration number are changed significantly, whereas in IV, an entirely different architecture space containing four-layer MLPs is used. From the table, it is quite evident that the effects of such major variations over the classification accuracy are insignificant. Therefore, any set of common PSO parameters within a reasonable range can be conveniently used within the proposed technique. Furthermore, for this ECG database, the choice of the architecture space does not affect the overall performance, yet any other ECG dataset containing more challenging ECG data might require the architecture spaces such as in IV in order to obtain a better generalization capability.

TABLE II
VEB AND SVEB CLASSIFICATION PERFORMANCE OF PROPOSED METHOD AND COMPARISON WITH THREE MAJOR ALGORITHMS FROM LITERATURE

Methods	VEB				SVEB			
	Acc	*Sen*	*Spe*	*Ppr*	*Acc*	*Sen*	*Spe*	*Ppr*
Hu et al. [11] [1]	94.8	78.9	96.8	75.8	N/A	N/A	N/A	N/A
Chazal et al. [15] [1]	96.4	77.5	98.9	90.6	92.4	76.4	93.2	38.7
Jiang and Kong [16] [1]	98.8	94.3	99.4	95.8	97.5	74.9	98.8	78.8
Proposed [1]	97.9	90.3	98.8	92.2	96.1	81.8	98.5	63.4
Jiang and Kong [16] [2]	98.1	86.6	99.3	93.3	96.6	50.6	98.8	67.9
Proposed [2]	97.6	83.4	98.1	87.4	96.1	62.1	98.5	56.7
Proposed [3]	98.3	84.6	98.7	87.4	97.4	63.5	99.0	53.7

[1] The comparison results are based on 11 common recordings for VEB detection and 14 common recordings for SVEB detection.

[2] The VEB and SVEB detection results are compared for 24 common testing records only.

[2] The VEB and SVEB detection results of the proposed system for all training and testing records.

TABLE III
VEB AND SVEB CLASSIFICATION ACCURACY OF PROPOSED METHOD FOR DIFFERENT PSO PARAMETERS AND ARCHITECTURE SPACES

(%)	I	II	III	IV
VEB	98.3	98.2	98.3	98.0
SVEB	97.4	97.3	97.1	97.4

I: $R^1_{\min} = \{11, 8, 4, 5\}, R^1_{\max} = \{11, 16, 8, 5\}, S=100, I=500$

II: $R^1_{\min} = \{11, 8, 4, 5\}, R^1_{\max} = \{11, 16, 8, 5\}, S=250, I=200$

III: $R^1_{\min} = \{11, 8, 4, 5\}, R^1_{\max} = \{11, 16, 8, 5\}, S=80, I=200$

IV: $R^1_{\min} = \{11, 6, 6, 3, 5\}, R^1_{\max} = \{11, 12, 10, 5, 5\}, S=400, I=500$

V. CONCLUSION

In this paper, we proposed an automated patient-specific ECG heartbeat classifier, which is based on an efficient formation of morphological and temporal features from the ECG data and evolutionary neural network processing of the input patterns individually for each patient. The TI-DWT and the PCA are the principal signal processing tools employed in the proposed feature extraction scheme. The wavelet-based morphology features are extracted from the ECG data and are further reduced to a lower dimensional feature vector using PCA technique. Then, by combining compact morphological features with the two critical temporal features, the resultant feature vector to represent each ECG heartbeat is used as the input to MLP classifiers, which are automatically designed (both network structure and connection weights are optimized) using the proposed MD-PSO technique.

With the proper adaptation of the native MD PSO process, the proposed method can thus evolve to the optimum network within an architecture space, and for a particular problem, according to a given error function. It is furthermore generic as it is applicable to any type of ANNs in an architecture space with varying size and properties, as long as a proper hash function enumerates all possible configurations in the architecture space with respect to their complexity into proper hash indexes representing the dimensions of the solution space over which an MD PSO process seeks for the optimal solution. MD PSO evolutionary process has a simple and unique structure for evolving ANNs without any significant parameter dependency or interference of any other method. It also has a native characteristic of having better

and faster convergence to optimum solution in low dimensions, and consequently, leads to *compact* networks.

The results of the classification experiments, which are performed over the benchmark MIT/BIH arrhythmia database, show that the proposed classifier technique can achieve average accuracies and sensitivities better than most of the existing algorithms for classification of ECG heartbeat patterns according to the AAMI standards. An overall average accuracy of 98.3% and an average sensitivity of 84.6% for VEB detection, and an average accuracy of 97.4% and an average sensitivity of 63.5% for SVEB detection were achieved over all 44 patient records from the MIT/BIH database. The overall results promise a significant improvement over other major techniques in the literature with the exception of the BbNN-based personalized ECG classifier in [16], which gave comparable results over the test set of 24 records. However, it used many critical parameters, BP and a specific ANN architecture, which may not suit feature vectors in higher dimensions. The proposed method is based only on well-known, standard techniques such as DWT and PCA, while using the most typical ANN structure, the MLPs. Experimental results approve that its performance is not affected significantly by variations of the few parameters used. Therefore, the resulting classifier successfully achieves the main design objectives, i.e., maintaining a robust and generic architecture with superior classification performance. As a result, it can be conveniently applied to any ECG database "as is," thus alleviating the need of human "expertise" and "knowledge" for designing a particular ANN.

APPENDIX

In an MD PSO process at time (iteration) t, each particle a in the swarm $\xi = \{x_1, \ldots, x_a, \ldots, x_S\}$ is represented by the following characteristics:

$xx_{a,j}^{xd_a(t)}(t)$: jth component (dimension) of the position in dimension $xd_a(t)$;

$vx_{a,j}^{xd_a(t)}(t)$: jth component (dimension) of the velocity in dimension $xd_a(t)$;

$xy_{a,j}^{xd_a(t)}(t)$: jth component (dimension) of the personal best (*pbest*) position in dimension $xd_a(t)$;

gbest(d): global best particle index in dimension d;

TABLE IV
PSEUDOCODE OF MD PSO ALGORITHM

MD PSO (*termination criteria:{IterNo,* ε_C *, ...},* $V_{\max}$ *,* $VD_{\max}$ *,* $D_{\min}, D_{\max}$)

1. For $\forall a \in [1, S]$ do:
    1.1.   Randomize $xd_a(0), vd_a(0)$
    1.2.   Initialize $\widetilde{xd}_a(0) = xd_a(0)$
    1.3.   For $\forall d \in [D_{\min}, D_{\max}]$ do:
        1.3.1.   Randomize $xx_a^d(0)$, $xv_a^d(0)$
        1.3.2.   Initialize $xy_a^d(0) = xx_a^d(0)$
    1.4.   End For.
2. End For.
3. For $\forall t \in [1, IterNo]$ do:
    3.1.   For $\forall a \in [1, S]$ do:
        3.1.1.   If ($f(xx_a^{xd_a(t)}(t)) < \min\left(f(xy_a^{xd_a(t)}(t-1), \min_{p \in S-\{a\}} \left(f(xx_p^{xd_a(t)}(t)) \right) \right)$) then do:
            3.1.1.1. $xy_a^{xd_a(t)}(t) = xx_a^{xd_a(t)}(t)$
            3.1.1.2.   If ($f(xx_a^{xd_a(t)}(t)) < f(xy_{gbest(xd_a(t))}^{xd_a(t)}(t-1))$) then $gbest(xd_a(t))=a$
            3.1.1.3.   If ($f(xx_a^{xd_a(t)}(t)) < f(xy_a^{\widetilde{xd}_a(t-1)}(t-1))$) then $\widetilde{xd}_a(t) = xd_a(t)$
            3.1.1.4.   If ($f(xx_a^{xd_a(t)}(t)) < f(x\hat{y}^{dbest}(t-1))$) then $dbest = xd_a(t)$
        3.1.2.   End If.
    3.2.   End For.
    3.3.   If the *termination criteria* are met, then **Stop**.
    3.4.   For $\forall a \in [1, S]$ do:
        3.4.1.   For $\forall j \in [1, xd_a(t)]$ do:
            3.4.1.1.   Compute $vx_{a,j}^{xd_a(t)}(t+1)$ using Eq. (6)
            3.4.1.2.   if($\left| vx_{a,j}^{xd_a(t)}(t+1) \right| > V_{\max}$) then clamp it to $\left| vx_{a,j}^{xd_a(t)}(t+1) \right| = V_{\max}$
            3.4.1.3.   Compute $xx_{a,j}^{xd_a(t)}(t+1)$ using Eq. (6)
        3.4.2.   End For.
        3.4.3.   Compute $vd_a(t+1)$ using Eq. (7)
        3.4.4.   if($\left| vd_a(t+1) \right| > VD_{\max}$) then clamp it to $\left| vd_a(t+1) \right| = VD_{\max}$
        3.4.5.   Compute $xd_a(t+1)$ using Eq. (7)
        3.4.6.   if($xd_a(t+1) < D_{\min}$) then $xd_a(t+1) = D_{\min}$)
        3.4.7.   if($xd_a(t+1) > D_{\max}$) then $xd_a(t+1) = D_{\max}$)
    3.5.   End For.
4. End For.

$x\hat{y}_j^d(t)$: jth component (dimension) of the global best position of swarm in dimension d;
$xd_a(t)$: dimension component;
$vd_a(t)$: velocity component of dimension;
$\widetilde{xd}_a(t)$: personal best dimension component.

Let f denote the dimensional fitness function that is to be optimized within a certain dimension range ($D_{\min} \leq N \leq D_{\max}$). Without loss of generality, assume that the objective is to find the minimum (position) of f at the optimum dimension within an MD search space. Assume that the particle a visits (back) the same dimension after T iterations (i.e., $xd_a(t) = xd_a(t+T)$), then the personal best position can be updated in iteration $t+T$ as follows:

$$
xy_{a,j}^{xd_a(t+T)}(t+T)
$$
$$
= \begin{cases} xy_{a,j}^{xd_a(t)}(t), & \text{if } f(xx_a^{xd_a(t+T)}(t+T)) \\ & \quad > f(xy_a^{xd_a(t)}(t)) \\ xx_{a,j}^{xd_a(t+T)}(t+T), & \text{else,} \end{cases},
$$
$$
j = 1, 2, \ldots, N. \qquad (4)
$$

Furthermore, the personal best dimension of particle a can be updated in iteration $t+1$ as follows:

$$x\tilde{d}_a(t+1) = \begin{cases} x\tilde{d}_a(t), & \text{if } f(xx_a^{xd_a(t+1)}(t+1)) \\ & > f(xy_a^{x\tilde{d}_a(t)}(t)), \\ xd_a(t+1), & \text{else} \end{cases}.$$

(5)

Recall that $gbest(d)$ is the index of the global best particle at dimension d and let $S(d)$ be the total number of particles in dimension d, then $x\hat{y}^{dbest}(t) = xy_{gbest(dbest)}^{dbest}(t) = \min(xy_1^{dbest}(t), \dots, xy_S^{dbest}(t))$. For a particular iteration t, and for a particle $a \in \{1, S\}$, first the positional components are updated in its current dimension $xd_a(t)$ and then the dimensional update is performed to determine its next $(t+1)$st dimension $xd_a(t+1)$. The positional update is performed for each dimension component $j \in \{1, xd_a(t)\}$ as follows:

$$\begin{aligned} vx_{a,j}^{xd_a(t)}(t+1) = {}& w(t)vx_{a,j}^{xd_a(t)}(t) + c_1 r_{1,j}(t) \\ & \times \left(xy_{a,j}^{xd_a(t)}(t) - xx_{a,j}^{xd_a(t)}(t) \right) + c_2 r_{2,j}(t) \\ & \times \left(x\hat{y}_j^{xd_a(t)}(t) - xx_{a,j}^{xd_a(t)}(t) \right) \\ xx_{a,j}^{xd_a(t)}(t+1) = {}& xx_{a,j}^{xd_a(t)}(t) + vx_{a,j}^{xd_a(t)}(t+1). \end{aligned}$$

(6)

Note that the particle's new position $xx_a^{xd_a(t)}(t+1)$ will still be in the same dimension $xd_a(t)$; however, the particle may fly to another dimension afterward with the following dimensional update equations:

$$\begin{aligned} vd_a(t+1) = {}& \left\lfloor vd_a(t) + c_1 r_1(t) \left(x\tilde{d}_a(t) - xd_a(t) \right) \right. \\ & \left. + c_2 r_2(t) (dbest - xd_a(t)) \right\rfloor \\ xd_a(t+1) = {}& xd_a(t) + vd_a(t+1) \end{aligned}$$

(7)

where $\lfloor \cdot \rfloor$ is the *floor* operator. Accordingly, the general pseudocode of the MD PSO method can be expressed as in Table IV.

To avoid arbitrary high values (i.e., exploding), thereby causing premature convergence [30], along with the (positional) velocity limit $V_{\max}$, two more clampings are applied for dimensional PSO components, such as $|vd_{a,j}(t+1)| < VD_{\max}$ and the initial dimension range set by the user $D_{\min} \le xd_a(t) \le D_{\max}$. Once the MD PSO process terminates, the optimum solution will be $x\hat{y}^{dbest}$ at the optimum dimension *dbest* achieved by the particle with the index *gbest(dbest)*, and finally, the best (fitness) score achieved will naturally be $f(x\hat{y}^{dbest})$.

REFERENCES

[1] R. Hoekema, G. J. H. Uijen, and A. v. Oosterom, "Geometrical aspects of the interindividual variability of multilead ECG recordings," *IEEE Trans. Biomed. Eng.*, vol. 48, no. 5, pp. 551–559, May 2001.

[2] K. Minami, H. Nakajima, and T. Toyoshima, "Real-time discrimination of ventricular tachyarrhythmia with Fourier-transform neural network," *IEEE Trans. Biomed. Eng.*, vol. 46, no. 2, pp. 179–185, Feb. 1999.

[3] L. Y. Shyu, Y. H. Wu, and W. C. Hu, "Using wavelet transform and fuzzy neural network for VPC detection from the holter ECG," *IEEE Trans. Biomed. Eng.*, vol. 51, no. 7, pp. 1269–1273, Jul. 2004.

[4] O. T. Inan, L. Giovangrandi, and G. T. A. Kovacs, "Robust neural-network-based classification of premature ventricular contractions using wavelet transform and timing interval features," *IEEE Trans. Biomed. Eng.*, vol. 53, no. 12, pp. 2507–2515, Dec. 2006.

[5] X. Alfonso and T. Q. Nguyen, "ECG beat detection using filter banks," *IEEE Trans. Biomed. Eng.*, vol. 46, no. 2, pp. 192–202, Feb. 1999.

[6] J. L. Willems and E. Lesaffre, "Comparison of multigroup logisitic and linear discriminant ECG and VCG classification," *J. Electrocardiol.*, vol. 20, pp. 83–92, 1987.

[7] J. L. Talmon, *Pattern Recognition of the ECG*. Berlin, Germany: Akademisch Proefscrift, 1983.

[8] D. A. Coast, R. M. Stern, G. G. Cano, and S. A. Briller, "An approach to cardiac arrhythmia analysis using hidden Markov models," *IEEE Trans. Biomed. Eng.*, vol. 37, no. 9, pp. 826–836, Sep. 1990.

[9] S. Osowski, L. T. Hoai, and T. Markiewicz, "Support vector machine based expert system for reliable heartbeat recognition," *IEEE Trans. Biomed. Eng.*, vol. 51, no. 4, pp. 582–589, Apr. 2004.

[10] Y. H. Hu, W. J. Tompkins, J. L. Urrusti, and V. X. Afonso, "Applications of artificial neural networks for ECG signal detection and classification," *J. Electrocardiol.*, vol. 26, pp. 66–73, 1994.

[11] Y. Hu, S. Palreddy, and W. J. Tompkins, "A patient-adaptable ECG beat classifier using a mixture of experts approach," *IEEE Trans. Biomed. Eng.*, vol. 44, no. 9, pp. 891–900, Sep. 1997.

[12] S. C. Lee, "Using a translation-invariant neural network to diagnose heart arrhythmia," in *Proc. IEEE Conf. Neural Inf. Process. Syst.*, Nov. 1989, pp. 240–247.

[13] P. de Chazal and R. B. Reilly, "A patient-adapting heartbeat classifier using ECG morphology and heartbeat interval features," *IEEE Trans. Biomed. Eng.*, vol. 53, no. 12, pp. 2535–2543, Dec. 2006.

[14] *Recommended Practice for Testing and Reporting Performance Results of Ventricular Arrhythmia Detection Algorithms*, Assoc. Adv. Med. Instrum., Arlington, VA, 1987.

[15] P. de Chazal, M. O'Dwyer, and R. B. Reilly, "Automatic classification of heartbeats using ECG morphology and heartbeat interval features," *IEEE Trans. Biomed. Eng.*, vol. 51, no. 7, pp. 1196–1206, Jul. 2004.

[16] W. Jiang and S. G. Kong, "Block-based neural networks for personalized ECG signal classification," *IEEE Trans. Neural Netw.*, vol. 18, no. 6, pp. 1750–1761, Nov. 2007.

[17] C. Li, C. X. Zheng, and C. F. Tai, "Detection of ECG characteristic points using wavelet transforms," *IEEE Trans. Biomed. Eng.*, vol. 42, no. 1, pp. 21–28, Jan. 1995.

[18] R. Silipo and C. Marchesi, "Artificial neural networks for automatic ECG analysis," *IEEE Trans. Signal Process.*, vol. 46, no. 5, pp. 1417–1425, May 1998.

[19] S. Osowski and T. L. Linh, "ECG beat recognition using fuzzy hybrid neural network," *IEEE Trans. Biomed. Eng.*, vol. 48, no. 11, pp. 1265–1271, Nov. 2001.

[20] M. Lagerholm, C. Peterson, G. Braccini, L. Edenbrandt, and L. Sörnmo, "Clustering ECG complexes using Hermite functions and self-organizing maps," *IEEE Trans. Biomed. Eng.*, vol. 47, no. 7, pp. 838–848, Jul. 2000.

[21] R. Silipo, P. Laguna, C. Marchesi, and R. G. Mark, "ST-T segment change recognition using artificial neural networks and principal component analysis," *Comput. Cardiol.*, pp. 213–216, 1995.

[22] X. Yao and Y. Liu, "A new evolutionary system for evolving artificial neural networks," *IEEE Trans. Neural Netw.*, vol. 8, no. 3, pp. 694–713, May 1997.

[23] T. Ince, S. Kiranyaz, and M. Gabbouj, "Automated patient-specific classification of premature ventricular contractions," in *Proc. IEEE Int. Conf. EMBS*, 2008, pp. 5474–5477.

[24] R. Mark and G. Moody, MIT-BIH Arrhythmia Database. (1997). [Online]. Available: http://ecg.mit.edu/dbinfo.html

[25] J. Pan and W. J. Tompkins, "A real-time QRS detection algorithm," *IEEE Trans. Biomed. Eng.*, vol. 32, no. 3, pp. 230–236, Mar. 1985.

[26] S. Mallat, *A Wavelet Tour of Signal Processing*, 2nd ed. San Diego, CA: Academic, 1999.

[27] S. G. Mallat and S. Zhong, "Characterization of signals from multiscale edges," *IEEE Trans. Pattern Anal. Mach. Intell.*, vol. 14, no. 7, pp. 710–732, Jul. 1992.

[28] N. V. Thakor, J. G. Webster, and W. J. Tompkins, "Estimation of QRS complex power spectra for design of a QRS filter," *IEEE Trans. Biomed. Eng.*, vol. BME-31, no. 11, pp. 702–705, Nov. 1984.

[29] S. Pittner and S. V. Kamarthi, "Feature extraction from wavelet coefficients for pattern recognition tasks," *IEEE Trans. Pattern Anal. Mach.*, vol. 21, no. 1, pp. 83–88, Jan. 1999.

[30] J. Kennedy and R. Eberhart, "Particle swarm optimization," in *Proc. IEEE Int. Conf. Neural Netw.*, vol. 4, Perth, W.A., Australia, 1995, pp. 1942–1948.

[31] F. Van Den Bergh, "An analysis of particle Swarm optimizers," Ph.D. dissertation, Dept. Comput. Sci., Univ. Pretoria, Pretoria, South Africa, 2002.

Moncef Gabbouj (M'85–SM'95) received the B.S. degree from Oklahoma State University, Stillwater, in 1985, and the M.S. and Ph.D. degrees from Purdue University, West Lafayette, Indiana, in 1986 and 1989, respectively, all in electrical engineering.

He is currently a Professor at the Department of Signal Processing, Tampere University of Technology, Tampere, Finland, where he was the Head of the Department during 2002–2007. During 2007–2008, he was a Visiting Professor at the American University of Sharjah, United Arab Emirates. His current research interests include multimedia content-based analysis, indexing, and retrieval; nonlinear signal and image processing and analysis; and video processing and coding. He was a Guest Editor of *Multimedia Tools and Applications* and the European journal *Applied Signal Processing*.

Prof. Gabbouj was a Distinguished Lecturer for the IEEE Circuits and Systems Society in 2004–2005. He has also been an Associate Editor of the IEEE TRANSACTIONS ON IMAGE PROCESSING. He is the past chairman of the IEEE Finland Section, the IEEE Circuits and Systems Society (CAS), the Technical Committee on DSP, and the IEEE Signal Processing (SP)/CAS Finland Chapter. He was a Senior Research Fellow of the Academy of Finland in 1997–1998 and 2007–2008. He was the recipient of the 2005 Nokia Foundation Recognition Award, and a co-recipient of the Myril B. Reed Best Paper Award from the 32nd Midwest Symposium on Circuits and Systems and the Nordic Signal Processing Symposium (NORSIG 94) Best Paper Award from the 1994 Nordic Signal Processing Symposium. He is a member of the IEEE SP and CAS societies.

Turker Ince received the B.S. degree from Bilkent University, Ankara, Turkey, in 1994, the M.S. degree from the Middle East Technical University, Ankara, in 1996, and the Ph.D. degree from the University of Massachusetts, Amherst (UMass-Amherst), in 2001, all in electrical engineering.

From 1996 to 2001, he was a Research Assistant at the Microwave Remote Sensing Laboratory, UMass-Amherst. He was a Design Engineer at Aware, Inc., Boston, MA, from 2001 to 2004, and at Texas Instruments Incorporated, Dallas, from 2004 to 2006. In 2006, he joined the faculty of the Computer Engineering Department, Izmir University of Economics, Izmir, Turkey, where he is currently an Assistant Professor. His current research interests include electromagnetic remote sensing and target recognition, radar signal processing, biomedical signal processing, neural networks, and global optimization techniques.
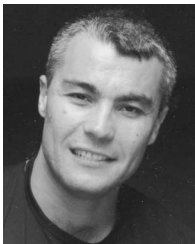
Serkan Kiranyaz was born in Turkey in 1972. He received the B.S. degree from the Electrical and Electronics Department, Bilkent University, Ankara, Turkey, in 1994, the M.S. degree in signal and video processing from Bilkent University in 1996, and the Ph.D. degree and the Docency from the Institute of Signal Processing, Tampere University of Technology, Tampere, Finland, in 2005 and 2007, respectively.

He was a Researcher at Nokia Research Center and later at Nokia Mobile Phones, Tampere, Finland. He is currently an Associate Professor at the Department of Signal Processing, Tampere University of Technology. His current research interests include multidimensional optimization, evolutionary neural networks, content-based multimedia indexing, browsing and retrieval algorithms, audio analysis and audio-based multimedia retrieval, object extraction, motion estimation and very low bit rate (VLBR) video coding, and MPEG4 over IP and multimedia processing.

Dr. Kiranyaz is an architect and the principal developer of the ongoing content-based multimedia indexing and retrieval framework, MUVIS.